J Control Autom Electr Syst
DOI 10.1007/s40313-014-0162-2

Rational Modeling of Nonhomogeneous Systems

Antonio C. S. Lima

Received: 25 April 2014 / Revised: 15 October 2014 / Accepted: 19 November 2014

Abstract Nonhomogeneous transmission systems occur in several practical configurations such as nonideally transposed overhead lines, cross-bonded cables, and river crossings of overhead lines. In the past, a compact and efficient representation of nonhomogeneous system (NhS) was only possible in the frequency domain as the chain matrix (matrix transfer function) was used to obtain an equivalent nodal admittance matrix. Time-domain representation of a NhS demands explicit representation of each homogeneous section, thereby not being an efficient solution. This work proposes to represent nonhomogeneous systems using a rational approximation which allows for a compact and accurate time-domain realization. In this approach, we exploit the fact that a NhS can be seen as a particular case of a frequency-dependent network equivalent. The frequency dependence of the NhS is included via the rational modeling of the admittance matrix using the so-called Vector Fitting algorithm. Two test cases are considered to illustrate the gain of the proposed solution. The first one is the modeling of a nonideally transposed transmission line, and the second one is a case of river crossing. To asses the accuracy of the modeling, the results are compared against the ones obtained either using the Numerical Laplace Transform and PSCAD.

Keywords Electromagnetic transients · Frequency response · Frequency-domain analysis · Network synthesis

1 Introduction

Nonhomogeneous systems (NhS) appear in a number of configurations such as cascade of slightly different lines, cross-bonded cables, or nonideally transposed overhead lines. In the past, the transient analysis of such systems was carried out in the frequency domain by the usage of the so-called chain matrix (Wedepohl and Indulkar 1974, 1975, 1979; Wedepohl 1997). This procedure allows for an efficient simulation and within reasonable system dimensions. It consists to derive an input–output relation between the terminals, and from this, multi-input multi-output transfer functions obtain an equivalent nodal admittance matrix $\mathbf{Y}_e$.

For time-domain simulations, however, the representation of such systems demands the inclusion of each homogeneous section, i.e., each untransposed line, cable segment. Consider for instance, the modeling of an nonideally transposed overhead line in time domain. One needs to include four line segments: two with one-sixth, and two with one-third of the total line length. Thus, the conventional modeling of a NhS in time domain implies an augmented system with some unnecessary data. However, if we could find a time-domain counterpart of the $\mathbf{Y}_e$, the explicit representation of the homogeneous section would be avoided, and a more efficient representation of a NhS in time domain would be obtained. Given the frequency-dependent nature of $\mathbf{Y}_e$, we could resort to a numerical Fourier (or Laplace) transform. To avoid dealing with the inverse transformation to obtain the impulse response, if the frequency dependence is synthesized via a rational model, i.e., using a common set of poles and residues matrices, then an efficient time-domain model can be obtained using recursive convolutions (Semlyen and Dabuleanu 1975) or trapezoidal integration (Noda 2005). In the Appendix, both procedures are summarized for a simple case. Time-domain electromagnetic transients (EMT) programs such as ATP, EMTP-RV, or PSCAD/EMTDC use a rational fitting in their frequency-dependent line models.

For the rational fitting, a procedure that is becoming increasingly more popular is the pole-relocating algorithm

A. C. S. Lima (✉)
Rio de Janeiro, Brazil
e-mail: acsl@dee.ufrj.br

Published online: 02 December 2014

known as Vector Fitting (VF) (Gustavsen and Semlyen 1999; Gustavsen 2006; Deschrijver et al. 2007). It is essentially a robust reformulation of the Sanathanan Koerner iteration (Gustavsen 2006). The VF algorithm was applied to transmission lines (Morched et al. 1999), wide-band transformer modeling (Gustavsen 2004), and frequency-dependent network equivalent (FDNE) (Gustavsen 2002). The latter can be adapted to represent a NhS as well as in a FNDE as there is no need to relate the block matrices. In all these applications, after the rational modeling is obtained, a post-processing stage is needed to ensure that a passive model is obtained (Semlyen and Gustavsen 2009; Gustavsen 2008).

The rational modeling of a nodal admittance matrix representing either a homogeneous system, as in the case of an overhead line or a NhS is a topic of intense research. While, for overhead lines, one might use the Folded Line Equivalent (Gustavsen and Semlyen 2009), for a NhS, the solution would be to adopt something similar to the Modal Vector Fitting, MVF (Gustavsen and Heitz 2008). One of the main disadvantages in the latter is the heavy computational burden and memory requirements. The goal of this paper is to propose a rational modeling of an equivalent nodal admittance matrix obtained via chain matrix allowing for efficient and compact time-domain realization of a NhS. It is an approach that has not been reported in the technical literature and can be seen as an alternative to the MVF and the more recent Mode-Revealing Transformation (Gustavsen 2014).

The paper is organized as follows: Sect. 2 reviews the modeling in both frequency and time domains of uniform and nonuniform overhead lines. The basic idea behind the use of the chain matrix is presented in Sect. 3. Section 4 presents the rational modeling of the admittance matrix of uniform and nonuniform lines. Section 5 presents the rational modeling of a nonideally transposed overhead line, being the case of a NhS obtained from a cascade of slightly different matrices. The second example is shown in Sect. 6 and consists of the time-domain modeling of an overhead line in a river crossing. Finally, Sect. 7 presents the main conclusions of this paper.

2 Line Modeling

As briefly mentioned, a NhS can be understood as a cascade of homogeneous lines. So, the first stage is to obtain the nodal admittance and the chain matrix associated with a single homogeneous configuration. In this section, we briefly review the frequency and time domains of a homogeneous line and how an equivalent nodal admittance matrix can be obtained in case of a nonuniform line.

2.1 Uniform Line

Consider an overhead line with n phases in the frequency domain. The relations of voltage and current along the line is given by the following differential equations:

$$\begin{aligned} \frac{\mathrm{d}^2\mathbf{V}}{\mathrm{d}x^2} &= \mathbf{Z}\,\mathbf{Y}\,\mathbf{V} \\ \frac{\mathrm{d}^2\mathbf{I}}{\mathrm{d}x^2} &= \mathbf{Y}\,\mathbf{Z}\,\mathbf{I} \end{aligned} \tag{1}$$

where the impedance per unit of length, $\mathbf{Z}$, and the admittance per unit of length, $\mathbf{Y}$, are complex symmetric matrices which are given as follows:

$$\begin{aligned} \mathbf{Z} &= \mathbf{Z}_i + \mathbf{Z}_e + \mathbf{Z}_s \\ \mathbf{Y} &= \mathbf{G} + j\omega\mathbf{P}^{-1} \end{aligned} \tag{2}$$

where $\mathbf{Z}_i$ is the internal impedance matrix, $\mathbf{Z}_e$ is the external impedance matrix considering an ideal medium (lossless), $\mathbf{Z}_s$ is the ground return impedance, $\mathbf{G}$ is the shunt conductance losses of the line, and $\mathbf{P}$ is the Maxwell Potential matrix. All matrices are per unit of length. Expressions for the impedance matrix and $\mathbf{P}$ can be found in Dommel (1992). $\mathbf{G}$ is a diagonal matrix with values obtained through measurements (Fernandes et al. 2004). For (1), it is assumed that all per unit of length parameters are constant for a given line length. A comparison of accuracy of approximate expressions typically used in transient analysis is given in Martins et al. (2005).

Each homogeneous segment can be associated with block symmetric matrices, as shown below:

$$\mathbf{Y}_n = \begin{bmatrix} \mathbf{Y}_s & \mathbf{Y}_m \\ \mathbf{Y}_m & \mathbf{Y}_s \end{bmatrix} \tag{3}$$

The block matrices in (3) are defined as

$$\begin{aligned} \mathbf{Y}_s &= \mathbf{Y}_c \left(\mathbf{I} + \mathbf{H}^2\right)\left(\mathbf{I} - \mathbf{H}^2\right)^{-1} \quad \text{and} \\ \mathbf{Y}_m &= -2\mathbf{Y}_c \left(\mathbf{I} - \mathbf{H}^2\right)^{-1} \end{aligned} \tag{4}$$

where $\mathbf{I}$ is a $n \times n$ identity matrix, with n being the number of conductors involved , $\mathbf{Y}_c = \mathbf{Z}^{-1}\sqrt{\mathbf{Z}\mathbf{Y}}$ is the characteristic admittance matrix, $\mathbf{H} = \exp(-\ell\sqrt{\mathbf{Z}\mathbf{Y}})$ is the propagation matrix also known as voltage deformation matrix and ℓ is the line length. The characteristic admittance and the propagation matrices can be obtained using modal decomposition or Schur decomposition. This allows for a phase-domain approach without resorting to modal decomposition (Lima and Portela 2007).

For the time-domain modeling, both $\mathbf{Y}_c$ and $\mathbf{H}$ need to be approximated by rational functions. For the former, the approximation has the form:

$$\mathbf{Y}_C \cong \sum_{i=1}^{N} \frac{\mathbf{R}_i}{s - a_i} + \mathbf{D} \tag{5}$$

where N is the fitting order, a_i are the poles obtained from fitting the trace of the characteristic admittance, $\mathbf{R}_i$ are the residue matrices, and $\mathbf{D}$ is a constant matrix. For the latter, the fitting is slightly different. First, the modal propagation time delay needs to be identified, so each mode h_i can be represented by a minimum phase-shift function $p_i(s)$ and a time delay τ_i, i.e.,

$$h_i \cong p_i(s)\, \exp(-s\tau_i) = \left(\sum_{n=1}^{N_i} \frac{\hat{c}_{ni}}{s + a_{ni}} \right) \exp(-s\tau_i) \tag{6}$$

where N_i is the fitting order of mode i, a_{ni} and $\hat{c}_{ni}$ are the poles and the residues. After identifying each τ_i (Bode 1945; Gustavsen 2004), modes with nearly equal time delays can be lumped together in an equivalent mode (Morched et al. 1999). Using the poles from the modes, each element H_{ij} of $\mathbf{H}$ is fitted with respect to the unknown residues $c_{ij_{mn}}$

$$H_{ij} \cong \sum_{m=1}^{K} \left(\sum_{n=1}^{N_i} \frac{c_{ij_{mn}}}{s + a_{mn}} \right) \exp(-s\tau_m) \tag{7}$$

where K is the number of collapsed modes, and τ_m is the collapsed time delay (Gustavsen 2008). One disadvantage of this approach is that the simulation time-step must be smaller than the smallest travel time τ_i. Therefore, if the homogeneous line section demands small line segments, a very small time-step for the time-domain analysis is needed.

2.2 Nonuniform Line

A nonuniform line (NUL) can be modeled in the frequency domain using the same voltage/current differential equation as uniform lines. The main difference is that both impedance and admittance matrices per unit length also vary along the line. Equation 8 shows the expressions defining the voltage and current vectors for a multiphase line.

$$\begin{aligned} \frac{\mathrm{d}^2\mathbf{V}}{\mathrm{d}x^2} &= -\left(\frac{\mathrm{d}\mathbf{Z}}{\mathrm{d}x}\mathbf{I} + \mathbf{Z}\frac{\mathrm{d}\mathbf{I}}{\mathrm{d}x} \right) \\ \frac{\mathrm{d}^2\mathbf{I}}{\mathrm{d}x^2} &= -\left(\frac{\mathrm{d}\mathbf{Y}}{\mathrm{d}x}\mathbf{V} + \mathbf{Y}\frac{\mathrm{d}\mathbf{V}}{\mathrm{d}x} \right) \end{aligned} \tag{8}$$

Unlike the uniform line, there is no analytic solution. In the past, finite differences have been used (Schelkunoff 1943), and numerical integration can be used (Semlyen 2003). In the latter, the time-domain implementation presented spurious oscillations (Ramirez et al. 2003) which emphasizes the importance of developing an accurate time-domain model of a NUL. That is why even more recent works such as Gomez et al. (2005) have focused on the frequency-domain analysis using the Numerical Laplace Transform to obtain the time responses for a NUL. Another possibility is to assume that $\mathbf{Z}$ and $\mathbf{Y}$ have an exponential dependency with respect to x. This procedure is commonly known as exponential line as has been applied to lossless lines (Oufi et al. 1994), lossy lines (AlFuhaid et al. 1998), and frequency-dependent tower models (Gutierrez et al. 2004; Nguyen et al. 1997).

An alternative procedure is the segmentation of the nonuniform line in smaller, pseudo-uniform lines. If the line is segmented in such a way that the variation along the line length in both $\mathbf{Z}$ and $\mathbf{Y}$ can be disregarded, this segment can be represented as a uniform line as described previously. If each uniform line is converted to the chain matrix, as briefly reviewed in the next section, it is possible to obtain an equivalent nodal admittance matrix for the whole nonuniform line.

The need for a small line length is one of the challenges for the representation of a nonuniform line in the time domain. As mentioned before, a small length line demands a very small time-step making the whole simulation unnecessarily heavy from the computational point of view. This is one of the reasons that a NUL is mainly simulated in frequency-domain analysis. Therefore, one of the main contributions of this work is to propose an accurate and efficient realization of a nonuniform line in time domain.

3 Chain Matrix

The structure of the nodal admittance matrix associated with a NhS is shown in (9). Here we opted to use the same notation as in Semlyen (2003).

$$\mathbf{Y}_{\mathrm{NhS}} = \begin{bmatrix} \mathbf{Y}_{SS} & \mathbf{Y}_{SR} \\ \mathbf{Y}_{RS} & \mathbf{Y}_{RR} \end{bmatrix} \tag{9}$$

A NhS is a passive symmetric element, so $\mathbf{Y}_{SR} = \mathbf{Y}_{RS}^T$ and unlike the homogeneous line section $\mathbf{Y}_{SS} \neq \mathbf{Y}_{RR}$. Thus, the system in (9) has the same structure of a FDNE. From $\mathbf{Y}_{\mathrm{NhS}}$, it is possible to derive a transfer matrix relating the voltage and current at terminals of the NhS. This is a generalization of the so-called quadrupole used for the analysis of positive sequence transmission lines. This transfer matrix, $\mathbf{Q}$, also known as the chain matrix (Wedepohl and Indulkar 1974) is shown in (10).

$$\mathbf{Q} = \begin{bmatrix} \mathbf{A} & \mathbf{B} \\ \mathbf{C} & \mathbf{D} \end{bmatrix} = \begin{bmatrix} -\mathbf{Y}_{RS}^{-1}\mathbf{Y}_{RR} & -\mathbf{Y}_{RS}^{-1} \\ \mathbf{Y}_{SR} - \mathbf{Y}_{SS}\mathbf{Y}_{RS}^{-1}\mathbf{Y}_{RR} & \mathbf{Y}_{SS}\mathbf{Y}_{RS}^{-1} \end{bmatrix} \tag{10}$$

The following relationships hold

$$\mathbf{A}\mathbf{D}^T - \mathbf{B}\mathbf{C}^T = \mathbf{I}, \qquad \mathbf{A}^T\mathbf{D} - \mathbf{C}^T\mathbf{B} = \mathbf{I} \tag{11}$$

where $\mathbf{I}$ is a $n \times n$ identity matrix. For homogeneous systems, $\mathbf{A} = \mathbf{D}$, only three matrices need to be calculated. From the transfer matrix, it is possible to obtain an equivalent nodal admittance matrix as shown below:

$$\mathbf{Y}_{n_{\mathrm{eq}}} = \begin{bmatrix} \mathbf{D}\mathbf{B}^{-1} & \mathbf{C} - \mathbf{D}\mathbf{B}^{-1}\mathbf{A} \\ -\mathbf{B}^{-1} & -\mathbf{B}^{-1}\mathbf{A} \end{bmatrix} \tag{12}$$

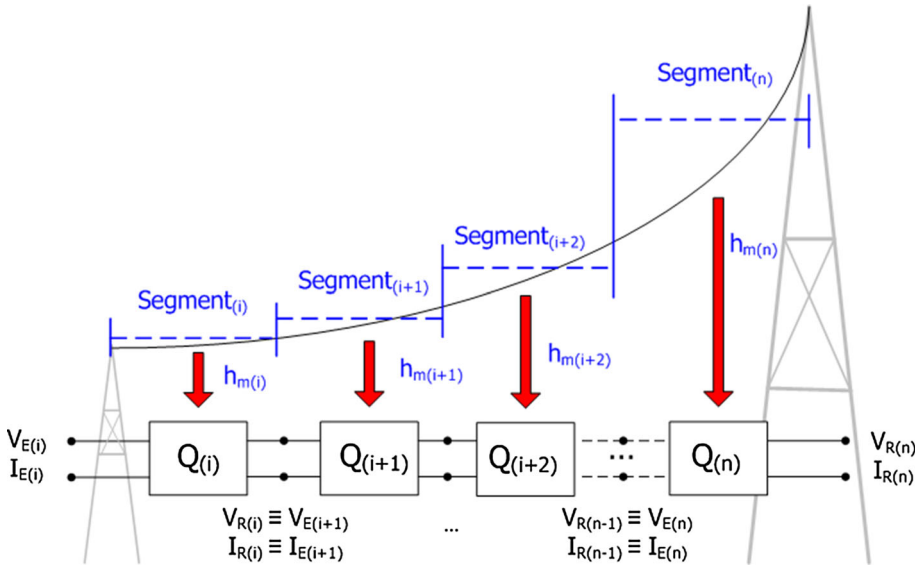

Fig. 1 Schematic representation of a nonuniform line with the chain matrix representation

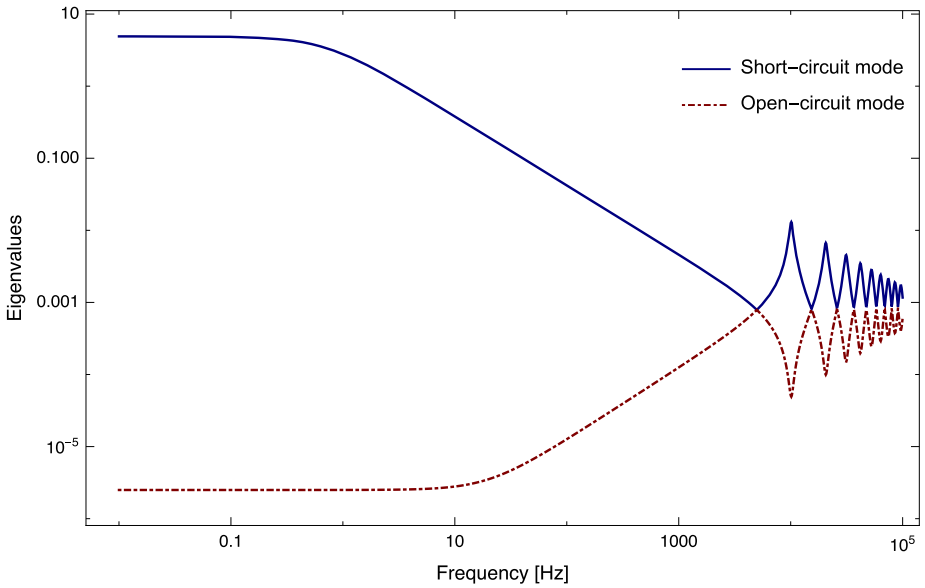

Fig. 2 Nodal admittance eigenvalue behavior for single-phase uniform line

As the nodal admittance above is symmetric, only three of blocks matrices need to be calculated as

$$\mathbf{C} - \mathbf{D}\mathbf{B}^{-1}\mathbf{A} = \left(-\mathbf{B}^{-1}\right)^{T} \tag{13}$$

To illustrate this procedure, consider the schematic representation of a nonuniform line as shown in Fig. 1. Each homogeneous section, i.e., with a constant height, is converted to a chain matrix. Then the cascade connection of all $\mathbf{Q}_i$ chain matrices leads to an equivalent matrix transfer function relating the voltage and current at both terminals of the NUL. Then by using (12), it is possible to obtain an equivalent nodal admittance matrix to be subjected to the rational approximation detailed in the next section.

4 Rational Modeling of Nodal Admittance Matrix

A possibility to overcome the time-step limitation in the time-domain modeling is to carry out a rational fitting of $\mathbf{Y}_n$. However, even in the case of a simple uniform line, there will be a large ratio between the largest and smallest eigenvalues given by the difference between short-circuit and open-circuit modes. To illustrate this, consider a single-phase overhead line with a length of 5 km. Figure 2 shows the absolute value of the two eigenvalues of $\mathbf{Y}_n$ using the formulation presented in Sect. 2. It can be seen that even in the lower frequency range, there is a large difference between them. The peaks in the short-circuit mode coincides with the minimum found in the open-circuit mode. This type of behavior is typical in the so-called stiff-systems and represents a challenge

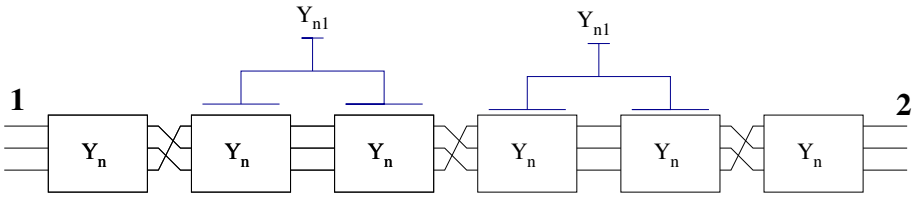

Fig. 3 Schematic representation of a nonideally transposed overhead line

for accurate representation using rational fitting, as an inaccurate representation of the smallest eigenvalues is expected. These inaccuracies can lead to large error amplifications in the time-domain responses, when high impedance terminal conditions are involved (Gustavsen and Semlyen 2009).

For uniform lines, one possibility to achieve a high accurate rational model is to use a Folded Line Equivalent (FLE) (Gustavsen and Semlyen 2009). The equivalent nodal admittance for this simple case is given by

$$\mathbf{Y}_{\text{FLE}} = \mathbf{K}^{-1}\mathbf{Y}_n\mathbf{K} = \begin{bmatrix} Y_s + Y_m & 0 \\ 0 & Y_s - Y_m \end{bmatrix} \tag{14}$$

where

$$\mathbf{K} = \begin{bmatrix} \mathbf{I} & \mathbf{I} \\ \mathbf{I} & -\mathbf{I} \end{bmatrix} \tag{15}$$

and $\mathbf{I}$ is an identity matrix. $\mathbf{K}$ in (15) is also known as the media and anti-media transformation matrix, and it has been used for modal-domain analysis of transmission lines (Tavares et al. 1999). Thus, a FLE decomposes the admittance matrix into two subsystems representing short-circuit ($Y_s - Y_m$) and open-circuit conditions ($Y_s + Y_m$). Each of this separate "modes" are then fitted independently considering that at a very high frequency both will asymptotically tend to the line characteristic admittance.

The extension of the FLE in the case of a NhS is not possible given the distinct structure. However, we may exploit some aspects of the FLE in order to derive the rational model for a NhS. First, we must assure that the NhS representation is asymptotically correct which can be achieved if

$$\mathbf{Y}_{\text{NhS}} = \overline{\mathbf{Y}}_C(\infty) + \mathbf{Y}_{\text{fit}}(\omega) \tag{16}$$

where $\overline{\mathbf{Y}}_C$ is a block diagonal matrix containing the real part of the characteristic admittance at infinite frequency as seen by each terminal of the NhS,

$$\overline{\mathbf{Y}}_C(\infty) = \begin{bmatrix} \Re\left(\mathbf{Y}_{c_1}(\infty)\right) & \mathbf{0} \\ \mathbf{0} & \Re\left(\mathbf{Y}_{c_2}(\infty)\right) \end{bmatrix} \tag{17}$$

where $\mathbf{Y}_{c_i}$ is the characteristic admittance at terminal i of the NhS.

In practice, we choose a very high frequency (100 MHz) to obtain those values. $\mathbf{Y}_{\text{fit}}$ stands for the part of the equivalent nodal admittance matrix that is to be fitted using rational functions, i.e.,

$$\mathbf{Y}_{\text{fit}}(\omega) \approx \sum_{m=1}^{N} \frac{\mathbf{R}_m}{j\omega - a_m} \tag{18}$$

the poles in (18) are obtained from fitting the trace of $(\mathbf{Y}_{\text{NhS}} - \overline{\mathbf{Y}}_C(\infty))$. As the trace of a matrix evenly contains information of all eigenvalues in $\mathbf{Y}_{\text{NhS}}$, we assumed that this would suffice for fitting all modes of a NhS. After the poles are obtained from the trace, the residue matrices are obtained establishing the rational model for $\mathbf{Y}_{\text{fit}}$. The rational model is applied to (18) using a zero constant term and inverse of the magnitude of each element as weighting. The model was obtained using the Matrix Fitting Toolbox (available at the Vector Fitting website: http://www.energy.sintef.no/Produkt/VECTFIT/index.asp.)

To ensure feasible simulations in time domain, it is needed to enforce the passivity of the rational approximation. For the passivity enforcement, we use the methodology proposed in Semlyen and Gustavsen (2009) which is an extension of the fast modal perturbation approach originally proposed in Gustavsen (2008).

5 Example: Nonideally Transposed Transmission Line

Figure 3 depicts a schematic representation of nonideally transposed overhead. Each $\mathbf{Y}_n$ stands for the admittance matrix of an untransposed overhead transmission line with one-sixth of the total line length. For the other line segments, we can calculate an admittance matrix $\mathbf{Y}_{n_1}$ related to the one-third of the total line length or treat it as a cascade connection of two $\mathbf{Y}_n$ without any transposition; this possibility is also depicted in Fig. 3.

Let $\mathbf{Q}$ be the chain matrix, i.e., transfer matrix, obtained through $\mathbf{Y}_n$ as shown in the previous section. The phase transposition then can be represented by a rotation matrix $\mathbf{R}$. For the phase transposition shown in Fig. 3, $\mathbf{R}$ is a block diagonal matrix given by

$$\mathbf{R} = \begin{bmatrix} \mathbf{R}_1 & \mathbf{0} \\ \mathbf{0} & \mathbf{R}_1 \end{bmatrix} \tag{19}$$

with $\mathbf{R}_1$ given by

$$\mathbf{R}_1 = \begin{bmatrix} 0 & 1 & 0 \\ 0 & 0 & 1 \\ 1 & 0 & 0 \end{bmatrix}, \tag{20}$$

and the transfer matrix for the whole line can then be assembled as shown below:

$$\mathbf{Q}_{\text{eq}} = \mathbf{Q} \cdot \mathbf{R} \cdot \mathbf{Q} \cdot \mathbf{Q} \cdot \mathbf{R} \cdot \mathbf{Q} \cdot \mathbf{Q} \cdot \mathbf{R} \cdot \mathbf{Q} = \begin{bmatrix} \mathbf{A}_{\text{eq}} & \mathbf{B}_{\text{eq}} \\ \mathbf{C}_{\text{eq}} & \mathbf{A}_{\text{eq}} \end{bmatrix} \tag{21}$$

The equivalent nodal admittance $\mathbf{Y}_{n_{\text{eq}}}$ can be obtained by applying (12) to the block matrices in (21).

To illustrate this procedure, consider a 300-km, and a 500-kV transmission lines. The conductor data are given in Appendix 1 . For the frequency-domain analysis to obtain the functions to be fitted, we have two options: either consider the cascade of 50-km lines and 100-km lines (as shown in Fig. 3) or using six sections of 50-km lines. We opted for the latter as we have found that the matrix multiplication was faster than calculating another nodal admittance matrix as the line length affects all the elements in the line nodal admittance matrix. The equivalent nodal admittance matrix was sampled using a combination of linearly and logarithmically space samples between 1 Hz and 10 kHz. Three thousand samples were used. This large number of samples is needed to resolve the frequency-domain functions. The nodal admittance of each section was obtained considering the skin effect in conductors and ground.

As in the case of nodal admittance matrix using the Folded Line Equivalent mentioned above, we have to force the approximated functions to be asymptotically correct. Thus, the functions to be fitted are in the form:

$$\mathbf{Y}_{n_{\text{eq}}} \approx \sum_{n=1}^{N} \frac{\mathbf{R}_n}{j\omega - a_n} + \overline{\mathbf{Y}}_C(\infty) \tag{22}$$

where $\overline{\mathbf{Y}}_C(\infty)$ is given by (17) with $\mathbf{Y}_{c_1} = \mathbf{Y}_{c_2}$. The poles and residues matrices' identification proceduress are the same as detailed in the previous section.

One hundred poles are used for the rational fitting, and only two passivity violations were found. Passivity enforcement was carried out using the methodology mentioned in the previous section. For this particular configuration, it was found that fewer poles would create less accurate fitting with larger passivity violations. On the other hand, increasing the number of poles did not affect the passivity violations, although some minor improvements in the quality of the fitting occurred.

The fitting results after passivity enforcement are shown in Fig. 4. The computer used is a Core 2 Duo 2,66 GHz with 4GB of RAM. The mismatches are some orders of magnitude below the fitted function. Table 1 summarizes the fitting results. It is worth mentioning that the passivity enforcement was only possible by using a 64-bits MATLAB. The 32-bits

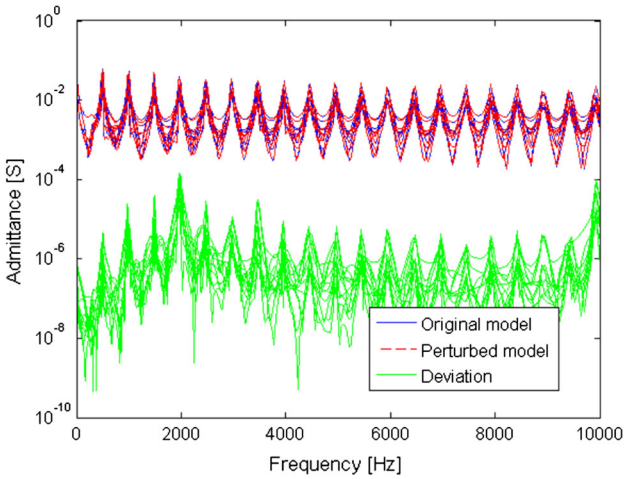

Fig. 4 Fitting results for a 300-km line, nonideally transposed 500-kV line

Table 1 Fitting results

Computer configuration	Fitting elapsed time (s)	Passivity assessment (s)	Passivity enforcement (s)
2,66 GHz C2D	34.7842	4.7386	88.9081

Table 2 ULM fitted poles

Length (km)	$\mathbf{Y}_c$	$\mathbf{h}_1$	$\mathbf{h}_2$	$\mathbf{h}_3$
50	11	7	7	6
100	11	8	7	6
300	10	9	9	–

version of the program failed to solve the passivity enforcement problem due to memory limitations.

For the time-domain analysis, we applied the trapezoidal integration to the state equation obtained with the rational model, see Appendix 2. Using this procedure, we can create a Norton equivalent that can be implemented in any EMT-type of program.

To compare the results, we also implemented the circuit as an ideally transposed and with a detailed representation of each line segment in PSCAD.

Table 2 summarizes the number of poles as function of the line length. The 300-km line was considered ideally transposed, and there are only two modes. We need at least four line models to represent the actual line: two for the 50-km and two for the 100-km segments. For this simulation, we used the so-called Universal Line Model (ULM) which is a phase coordinate model implemented in PSCAD. For the frequency-domain fitting of both the characteristic admittance and propagation functions, a maximum frequency of 1 MHz was used. In the NhS simulation, we were able to limit the frequency up to 10 kHz.

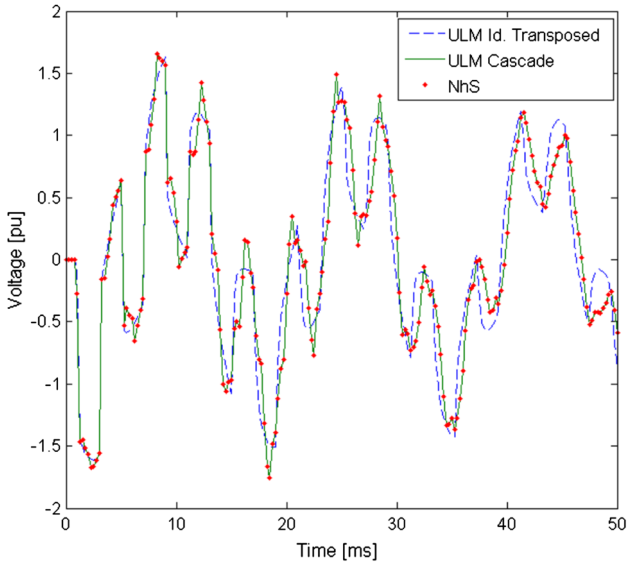

Fig. 5 Time-domain response for a simple three-phase energization

Figure 5 shows the time-domain responses, considering these three approaches: cascade of ULMs, a NhS, and an ideally transposed line. From the results, we can see that there are some noticeable differences between the ideally transposed and the other two models. The NhS presented a very good agreement with the ones from detailed time-domain simulation, i.e., using ULM. Although a direct comparison is not valid, we note that the explicit representation of each line segmented led to a simulation where 128 poles were needed. The simulation of the NhS needed 100 poles and has a far narrower frequency band. Therefore, it seems that a NhS provides a small but significant gain compared with the conventional approach.

To illustrate that the gain of using NhS can be even more pronounced, we consider a case of a 500-kV line with shunt compensation using line reactors. These reactos are used to reduce the line charging. In some countries like Brazil, most of the 500-kV lines have greater than 250 km line reactors. These reactors are supposed to be in operation as long as the line operates. In the actual 500-kV circuits using the configuration presented here, the so-called compact lines, the level of shunt reactive power compensation may be in the range from 80 % to almost 100 %.

In the case of shunt reactor connected to the line, the equivalent chain matrix can be obtained by

$$\mathbf{Q}_{\mathrm{eq}_{\mathrm{comp}}} = \mathbf{Q}_y \cdot \mathbf{Q}_{\mathrm{eq}} \cdot \mathbf{Q}_y \tag{23}$$

where $\mathbf{Q}_y$ is defined by

$$\mathbf{Q}_y = \begin{bmatrix} \mathbf{I} & \mathbf{0} \\ \mathbf{Y}_L & \mathbf{I} \end{bmatrix} \tag{24}$$

and $\mathbf{Y}_L$ is a diagonal matrix for the shunt reactor. In conventional EMT-type modeling, the frequency dependency of the shunt reactor would also demand a rational model. Although if the chain matrix is used, the frequency dependency can be included directly in the equivalent model. Naturally, the procedure to obtain the equivalent nodal admittance matrix is the same as before.

Table 3 Fitting results for compensated line

Computer configuration	Fitting elapsed time (s)	Passivity assessment (s)	Passivity enforcement (s)
2,66 GHz C2D	35.0067	4.5728	88.4902

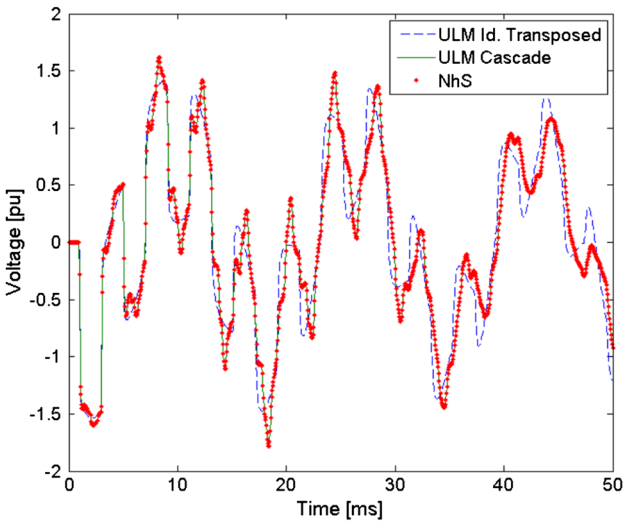

Fig. 6 Time-domain response for a simple three-phase energization of compensated line

For this configuration even if we consider the frequency dependence of the line reactor, it is possible to fit the equivalent nodal admittance matrix using 100 poles. The timing for the fitting and the passivity enforcement are almost the same as before. Thus, the inclusion of the shunt admittance did not impact the overall modeling.

The fitting procedure was able to include this external element without compromising its performance. Table 3 summarizes the timings. Figure 6 depicts the time-domain responses for the three modeling. Once again, there is a very good agreement between the detailed modeling using ULM and the representation of the shunt admittance and the one we obtained using a NhS. Again from the results, we see that there are some noticeable differences between the ideally transposed line and the NhS. The NhS results are in very good agreement to those from the detailed ULM model.

6 Example: River Crossing of Overhead Transmission Line

Typically, an overhead line at voltage level equal or higher than 230 kV has an average span of 300 m up to 400 m. How-

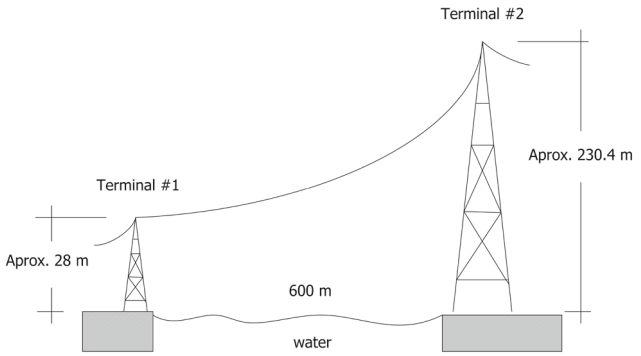

Fig. 7 River crossing test case

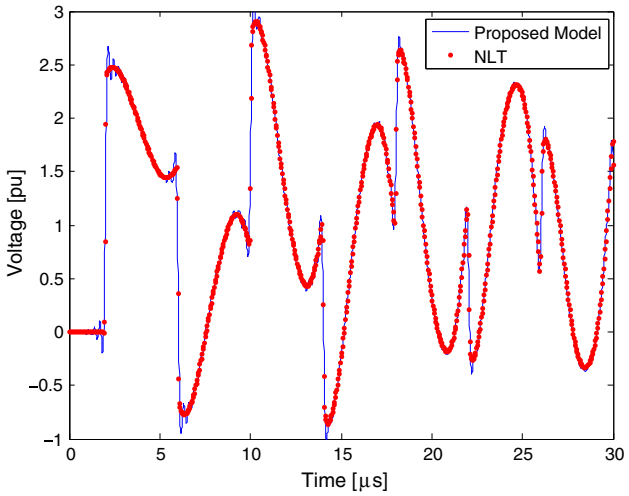

Fig. 8 Voltage at the first phase of terminal #2 for a step voltage at terminal #1

ever, in the case of a river crossing, the span might be longer, and higher towers are needed. One possible configuration for a river crossing is shown in Fig. 7. It is essentially the same configuration as in Semlyen (2003), Gomez et al. (2005). It is a horizontal ("flat") line where adjacent conductors are 10 m apart. The conductor radius is 2.54 cm. The water resistivity is 10 Ωm.

As mentioned in this paper, the first issue is to determine the length of the uniform line used for segmentation. It is possible to use the Courant–Friedrichs–Lewvy (CFL) criterion as in Gomez et al. (2005). Here we opted for a different proposition. In each segment, we calculate the finite-length impedance using the expressions presented in Ametani et al. (1994), Ametani (2002). This result is compared with the one using conventional line parameter expressions. The length of the segment should be such that the difference between both formulations does not exceed 0.1 %. This result indicated a maximum length about 20 m. It is worth mentioning that the results are in the same order of magnitude; using CFL, we had a segment length of 30 m. Another possible criterion would be the comparison with the cylindrical electrode formulation (Salari Filho and Portela 2007). This comparison is left for future research.

Traditionally, the height of a conductor can be determined using the parabolic approximation of the catenary. However, it was found that in case of very wide spans, there can be some noticeable differences. Therefore, it was decided to use the catenary equation where the height of a conductor along the span is given by

$$y = q\left(\cosh\left(\frac{x}{q}\right) - 1\right) \tag{25}$$

where q is the "specific weight" of the conductor. Thus, phase-conductors will present distinct sags compared with ground wires. The constant height of conductors to be used in each segment Q_i is obtained by the integration of (25), leading to

$$\overline{y} = q + \frac{q^2\left(\sinh\left(\frac{x_1}{q}\right) - \sinh\left(\frac{x_0}{q}\right)\right)}{x_1 - x_0} \tag{26}$$

where x_1 and x_0 are the x-coordinates that define the length of the uniform line approximation.

After obtaining the chain matrix for each segment, a simple multiplication allows one to obtain the equivalent transfer matrix for the whole system which is then converted to an equivalent nodal admittance matrix. Thus, the procedure is the same as in the previous example, although the values involved are rather different.

For the rational model realization we must first calculate $\overline{\mathbf{Y}}_C(\infty)$ as in (17) using the line segments closest to each terminal, i.e., with $\mathbf{Y}_{c_1}$ as the characteristic admittance of the line segment closest to terminal #1 and $\mathbf{Y}_{c_2}$ being the one related to terminal #2. Unlike the previous case, $\mathbf{Y}_{c_2} \neq \mathbf{Y}_{c_1}$ given the difference in conductor's height at each terminal. For the rational model, we had to consider 90 poles. Eight passivity violations were found although an overall passive model was obtained using the passivity enforcement procedure mentioned above.

For the time response, we consider a step voltage of 1 V applied at terminal #1, while terminal #2 remains open. Figure 8 shows the output on the outside phase conductor at terminal #2 obtained using the proposed procedure and with the Numerical Laplace Transform. If this curve is compared with Fig. 11 in Ramirez et al. (2003), there seems to be a considerable agreement but without the spurious oscillations.

It is important to notice that as this case is simulated in an EMT-type of program (PSCAD), a time-step below 60 ns is needed for 20-m line segments. If instead the line segments of 30 m are considered, the time-step would be smaller than 100 ns. However, using a NhS modeling, we were able to simulated the system considering segments of 20 m and with

Table 4 Mismatch in voltages as function of the number N of chain matrices

N	ℓ	Max(ΔV)
20	30	0.0238651
30	20	0
40	15	0.00679813

a time-step of 500 ns. This shows that an important gain in computational time is gained without significant loss of accuracy compared with a NhS modeling in the frequency domain.

This case was also used to assess the voltage mismatches as a function of the number of chain matrices used to obtain the NUL equivalent. The case using 30 chain matrices is used as a base of comparison. Table 4 summarizes this comparison where N is the number of chain matrices, l is the length of the uniform line segment, and Max(ΔV) stands for the maximum voltage mismatch found in the time-domain simulations.

7 Conclusions

In this paper, we presented an approach for efficient time-domain modeling of NhS using rational modeling. This approach allows for an efficient and compact representation of the system under analysis without explicit modeling of the homogeneous system. Such approach was widely used in the analysis of transients using frequency-domain techniques, i.e., NLT, although being limited mostly to linear systems. The time response showed both stable and accurate response compared with the results obtained using the NLT. The results also indicated that the higher the nonhomogeneity between uniform line sections, the better the improvement when using a rational modeling of the whole NhS. Further developments are expected to evaluate the behavior of NhS in the time domain when a nonlinear device is involved in such a surge arrester. There is also a need for the development of an identification algorithm to improve the sectioning of NUL in order to obtain the best possible system (i.e, with the highest accuracy possible) and the minimum order of homogeneous sections.

Appendix 1: Overhead Line Conductor Data

For the 500-kV lines, each phase has a four-conductor bundle with a 0.5-m spacing, phase conductors are Rail, and ground wires are 3/8" EHS. The coordinates for the centers of phase conductors bundle and for the ground wires are given as follows:

$$\begin{aligned} x &= [-4.5 \quad 0 \quad 4.5 \quad -3.5 \quad 3.5] \\ y &= [11 \quad 15.5 \quad 11 \quad 26 \quad 26] \end{aligned} \tag{27}$$

Appendix 2: State Space Formulation

For a first-order proper pole-residue model with input u and output y, we may write in the frequency domain:

$$y = \left(\frac{r}{s-a} + d\right) u \tag{28}$$

in the time domain (28) can be written as

$$\begin{aligned} \dot{x} &= a\,x + r\,u \\ y &= r\,x + d\,u \end{aligned} \tag{29}$$

a discrete time model of (29) can be obtained using either trapezoidal rule integration or recursive convolution. The expressions are shown in (30).

$$\begin{aligned} x(n) &= \alpha\,x(n-1) + (\alpha\lambda + \mu)\;u(n-1) \\ y(n) &= x(n) + (\lambda + d)\;u(n) \end{aligned} \tag{30}$$

If the trapezoidal integration rule is applied, then the coefficients α, λ and μ are given by

$$\alpha = \frac{2 + a\,\Delta t}{2 - a\,\Delta t} \qquad \lambda = \mu = \frac{r\,\Delta t}{2 - a\,\Delta t} \tag{31}$$

and in the case where recursive convolutions are used, we have

$$\begin{aligned} \alpha &= \exp(a\,\Delta t) \qquad \lambda = -\frac{r}{a}\left(1 + \frac{1-\alpha}{a\,\Delta t}\right) \\ \mu &= \frac{r}{a}\left(\alpha + \frac{1-\alpha}{a\,\Delta t}\right) \end{aligned} \tag{32}$$

References

AlFuhaid, A., Oufi, E., & Saied, M. (1998). Application of nonuniform-line theory to the simulation of electromagnetic transients in power systems. *International Journal Electric Power and Energy System*, *20*(3), 225–233.

Ametani, A. (2002). Wave propagation on a nonuniform line and its impedance and admittance. *The Science and Engineering Review of Doshisa University*, *43*(2), 11–23.

Ametani, A., Kasai, Y., & Sawada, J. (1994). Frequency-dependent impedance of vertical conductor and a multiconductor tower model. *Proceeding IEE Generation Transmission and Distribution*, *141*(4), 339–345.

Bode, H. W. (1945). *Network analysis and feedback amplifier design*. New York: D. Van Nostrand.

Deschrijver, D., Gustavsen, B., & Dhaene, T. (2007). Advancements in iterative methods for rational approximation in the frequency domain, *IEEE Transactions on Power Delivery*, p. 2006.

Dommel, H. (1992). *EMTP theory book*. Vancouver: MicroTran Power System Analysis Corporation.

Fernandes, A. B., Neves, W. L. A., Costa, E. G., & Cavalcanti, M. N. (2004). Transmission line shunt conductance from measurements. *IEEE Transactions on Power Delivery*, *19*(2), 722–728.

Gomez, P., Moreno, P., & Naredo, J. (2005). Frequency domain transiente analyis of nonuniform lines with incident field excitation. *IEEE Transactions on Power Delivery*, *20*(3), 2273–2280.

Gustavsen, B. (2002). Rational approximation of frequency dependent admittance matrices. *IEEE Transactions on Power Delivery*, *17*(4), 1093–1098.

Gustavsen, B. (2004). Wide band modeling of power transformers. *IEEE Transactions on Power Delivery*, *19*(1), 414–422.

Gustavsen, B. (2006). Improving the pole relocation properties of vector fitting. *IEEE Transactions on Power Delivery*, *21*(3), 1587–1592.

Gustavsen, B. (2008). Fast passivity enforcement for pole-residue models by perturbation of residue matrix eigenvalues. *IEEE Transactions on Power Delivery*, *23*(3), 2278–2285.

Gustavsen, B. (2014). Rational modeling of multiport systems via a symmetry and passivity preserving mode-revealing transformation. *IEEE Transactions on Power Delivery*, *29*(1), 199–206.

Gustavsen, B., & Heitz, C. (2008). Modal vector fitting: A tool for generating rational models of high accuracy with arbitrary terminal conditions. *IEEE Transactions on Advanced Packaging*, *31*(4), 664–672.

Gustavsen, B., & Semlyen, A. (1999). Rational approximation of frequency domain responses by vector fitting. *IEEE Transactions on Power Delivery*, *14*(3), 1052–1061.

Gustavsen, B., & Semlyen, A. (2009). Admittance-based modeling of transmission lines by a folded line equivalent. *IEEE Transactions on Power Delivery*, *24*(1), 231–239.

Gutierrez, R., Moreno, P., Naredo, J., Bermudez, J.-L., Paolone, M., Nucci, C., et al. (2004). Nonuniform transmission tower model for lightning transient studies. *IEEE Transactions on Power Delivery*, *19*(2), 490–496.

Lima, A. C. S., & Portela, C. (2007). Inclusion of frequency-dependent soil parameters in transmission-line modeling. *IEEE Transactions on Power Delivery*, *22*(1), 481–491.

Martins, T. F. R. D., Lima, A. C. S., & Carneiro, S. Jr., (2005). Effect of impedance approximate formulae on frequency dependence realization. In *Proceeding of IPST'05 - International on Power System Transients Conference*, Montreal.

Morched, A., Gustavsen, B., & Tartibi, M. (1999). A universal model for accurate calculation of electromagnetic transients on overhead lines and underground cables. *IEEE Transactions on Power Delivery*, *14*(3), 1032–1038.

Nguyen, H., Dommel, H., & Marti, J. (1997). Modeling of single-phase nonuniform transmission lines in electromagnetic transient simulations. *IEEE Transactions on Power Delivery*, *12*, 916–921.

Noda, T. (2005). Identification of a multiphase network equivalent for electromagnetic transient calculations using partitioned frequency response. *IEEE Transactions on Power Delivery*, *20*(2), 1134–1142.

Oufi, E., AlFuhaid, A., & Saied, M. (1994). Transient analysis of lossless single-phase nonuniform transmission lines. *IEEE Transactions on Power Delivery*, *9*, 1694–1700.

Ramirez, A., Semlyen, A., & Iravani, R. (2003). Modeling nonuniform transmission lines for time domain simulation of electromagnetic transients. *IEEE Transactions on Power Delivery*, *18*(3), 968–974.

Salari Filho, J., & Portela, C. (2007). A methodology for electromagnetic transients calculation-an application for the calculation of lightning propagation in transmission lines. *IEEE Transactions on Power Delivery*, *22*(01), 527–536.

Schelkunoff, S. (1943). *Electromagnetic waves*. New York: D. Van Nostrand Co.

Semlyen, A. (2003). Some frequency domain aspects of wave propagation on nonuniform lines. *IEEE Tranactions on Power Delivery*, *18*(1), 315–322.

Semlyen, A., & Dabuleanu, A. (1975). Fast and accurate switching transient calculations on transmission lines with ground return using recursive convolutions. *IEEE Transactions on Power Apparatus and Systems*, *94*, 561–571.

Semlyen, A., & Gustavsen, B. (2009). A half-size singularity test matrix for fast and reliable passivity assessment of rational models. *IEEE Transactions on Power Delivery*, *24*(1), 345–351.

Tavares, M., Pissolato, J., & Portela, C. (1999). New multiphase mode domain transmission line model. *International Journal of Electrical Power and Energy Systems*, *21*(4), 585–601.

Wedepohl, L. (1997). The theory of natural modes in multiconductor transmission systems, the University of British Columbia. Rep: Tech.

Wedepohl, L., & Indulkar, C. (1974). Wave propagation in nonhomogeneous systems. Properties of the chain matrix. *Proceedings of the IEE*, *121*(9), 997.

Wedepohl, L., & Indulkar, C. (1975). Switching overvoltages in short crossbonded cable systems using the Fourier transform. *Proceedings of IEE*, *122*(11), 1217–1221.

Wedepohl, L., & Indulkar, C. (1979). Switching overvoltages in long crossbonded cable systems using the Fourier transform. *IEEE Transactions on PAS*, *PAS–98*, 1476–1480.